,

MULTI-LAYER HEALTH-AWARE ECONOMIC PREDICTIVE CONTROL OF A PASTEURIZATION PILOT PLANT

FATEMEH KAEIMI POUR [a], VICENC PUIG [a,*], CARLOS OCAMPO-MARTINEZ [a]

[a] Automatic Control Department, Universitat Politècnica de Catalunya
Institut de Robòtica i Informàtica Industrial (CSIC-UPC), C/. Llorens i Artigas 4-6, 08028 Barcelona, Spain
e-mail: {fkarimi, vpuig, cocampo}@iri.upc.edu

This paper proposes two different health-aware economic predictive control strategies that aims minimizing the damage of components in a pasteurization plant. The damage is assessed with the rainflow-counting algorithm that allows to estimate the components fatigue. By using the results obtained from this algorithm, a simplified model that characterizes the health of the system is developed and integrated into the predictive controller. The overall control objective is modified by adding an extra criterion that takes into account the accumulated damage. The first strategy is a single-layer predictive controller with integral action to eliminate the steady-state error that appears when adding the extra criterion. In order to achieve the best minimal accumulated damage and operational costs, the single-layer approach is improved with a multi-layer control scheme, where the solution of the dynamic optimization problem is obtained from the model in two different time scales. Finally, to achieve the advisable trade-off between minimal accumulated damage and operational costs, both control strategies are compared in simulation over a utility-scale pasteurization plant.

Keywords: model predictive control, two-layers control scheme, fatigue, economic optimization, health-aware controller

1. Introduction

One of the most important food preservation techniques is pasteurization, which is widely used in food industries. The pasteurization process implies applying heat to some products such as milk, cream, beer and others. Mainly, pasteurization implies that a food product is exposed to some temperature profile during a predetermined period of time, in order to reduce the proportion of microorganisms. This process is distributed into three sections that involve heating, cooling and regeneration treatments. The most important treatment is heating, which involves heat exchanger equipment to heat up the temperature of the product at requested setpoint, and then maintaining this temperature during a constant time. Among many pasteurization approaches, the High-Temperature Short-Time (HTST) approach is generally accepted as the industry standard (Alastruey *et al.*, 1999). In this process, the time temperature compound can change depending on the product and some of its properties as viscosity, fat percentage, solid residues, among others. Controlling and maintaining the temperature of the process are key aspects in the pasteurization process. Particularly, in the case of milk pasteurization, the heating temperature is in general from 72°C to 74°C during 15 - 20 s followed by cooling (Khadir, 2011). Hence, a suitable control strategy for the system needs to be designed in order to manage the product temperature for keeping the desired product quality. The necessity of a significant control of the process arises from the savings in energy, product and time if an accurate tracking of the setpoint is performed. On the other hand, due to the high number of load cycles that occur during the life of a pump within a pasteurization process, its fatigue estimation is an important factor for the proper control of such processes. For this reason, research regarding the integration of control with a fatigue-based prognosis of components has been developed in recent years. Fatigue leads to the breakdown of the material subject to stress, especially when frequent series of stresses are applied (Osgood, 2013). Damage has been widely and exhaustively studied from different perspectives (Musallam and Johnson, 2012). In this paper, the Palmgren-Miner linear damage rule is used to perform fatigue analysis (Miner et al., 1945). This rule, commonly

*Corresponding author

called the Miner's rule, is being currently used throughout the industry and in academia (Marin *et al.*, 2008).

Among the last decades, model-based predictive control (MPC) has had a significant impact on industrial control engineering because of its ability to deal with multivariable control, constraints and delays on system variables and actuators (Hrovat *et al.*, 2012; Yetendje *et al.*, 2012). Also, MPC has started to attract the attention of both academia and industry due to the possibility of dealing with the conflicting power optimization and fatigue load reduction (Körber, 2014). Furthermore, a pasteurization system includes typical behaviors of relevant processes, such as complex dynamical models with nonlinearities, which imply important challenges when a suitable controller should be designed. In the literature, there are different modeling approaches and controller strategies for pasteurization systems. In Ibarrola *et al.* (1998), the complete process model leads to a multivariable first order with delay transfer functions of varying parameters after decomposing the system into functional subsystems. Other models from the whole system and/or some subsystems are obtained in (Aadaleesan *et al.*, 2008; Mokhtar *et al.*, 2012). Regarding pasteurization process control, in Ibarrola *et al.* (2002), a Dynamic Matrix Control (DMC) is designed and implemented by using the system models proposed in Ibarrola *et al.* (1998). Mokhtar *et al.* (2012) proposed a scheme based on PID controllers with different tuning methods. The regulation of both water and milk temperatures by using MPC is reported in Niamsuwan *et al.* (2014), where transient behaviors have been suitably handled with respect to other control techniques such as cascade generic model control (GMC) strategy. Rosich and Ocampo-Martinez (2015) provided three different control topologies based on MPC that aim to the minimization of the energy consumption. A recent study by Karimi Pour, Ocampo-Martinez and Puig (2017) involved a output-feedback MPC controller based on Linear Parameter Varying (LPV) model of the pasteurization system.

On the other hand, MPC has been recently proved as an adequate strategy for implementing health-aware control schemes. A data-based MPC strategy that incorporates fatigue estimation was presented in de Jesus Barradas-Berglind *et al.* (2015). In the work of Odgaard *et al.* (2015), an approach including dynamic inflow into the MPC controller is proposed to decrease fatigue load. Several economic-oriented controllers have been recently proposed within the MPC framework (Ellis *et al.*, 2014; Grosso *et al.*, 2016; Lobos and Momot, 2002) but without considering safety issues of the system components. In fact, both safety stock and actuator lifetime are competing with the economic performance of the system. For this reason, it is required to have a flexible control strategy that allows to trade off the economic optimization and the safety of the system.

This paper presents a health-aware control (HAC) with economic objectives that considers the information about the system health to adapt the objectives of the control law to extend the remaining useful life (RUL) of the considered system. Thus, the control inputs are generated to fulfill the control objectives/constraints but at the same time to extend the lifespan of the system components. In this way, the HAC makes an effort to attain maximum performance while not degrading the system too much. In case that the controller is implemented using MPC, the trade-off is based on modifying the control objective including new terms that take care of the system health. This leads to solving a multi-objective optimization problem where a trade-off between system health and performance should be established (Sanchez *et al.*, 2015).

The main contribution of this paper consists in the design of an improved health-aware economic MPC strategy. This strategy minimizes the damage of the pasteurization components and reduces the power consume of the electrical heater as economic objective, while still the pasteurization temperature tracks the suitable references related to the products, extending the result presented in Karimi Pour, Puig and Ocampo-Martinez (2017). The novelty of this paper is a multi-layer scheme including the health-aware and economic operation that extends and improves the preliminary ideas presented in Karimi Pour, Puig and Ocampo-Martinez (2017). The upper layer solves an optimization problem with an economic cost function and a new objective to minimize the accumulated damage at slow time scales. In the lower layer, a linear MPC controller forces the process dynamics to track the trajectory provided by the upper layer. Finally, a comparison between the multi-layer and single-layer control schemes is performed by using a high-fidelity simulator of a utility-scale pasteurization plant.

The remainder of the paper is organized as follows. Section 2 briefly describes the pasteurization processes and the MPC problem statement. Section 3 presents the fatigue analysis applied to the pasteurization system. In Section 4, two health-aware MPC control schemes are presented. Section 5 presents the case study where the effectiveness of the proposed approaches is simulated as well as a comparative study. Finally, in Section 6, the conclusions are drawn and some research lines for future work are proposed.

Notation 1 *Throughout this paper,* $\mathbb{R}, \mathbb{R}^n, \mathbb{R}^{m\times n}, \mathbb{R}_+$ *denote the field of real numbers, the set of column real vectors of length* n*, the set of* m *by* n *real matrices and the set of non-negative real numbers, respectively. Similarly,* $\mathbb{Z}_+$ *denotes the set of non-negative integer numbers including zero. Besides,* $\mathbb{Z}_{[a,b]} := \{x \in \mathbb{Z}_+ | a \leq x \leq b\}$ *for*

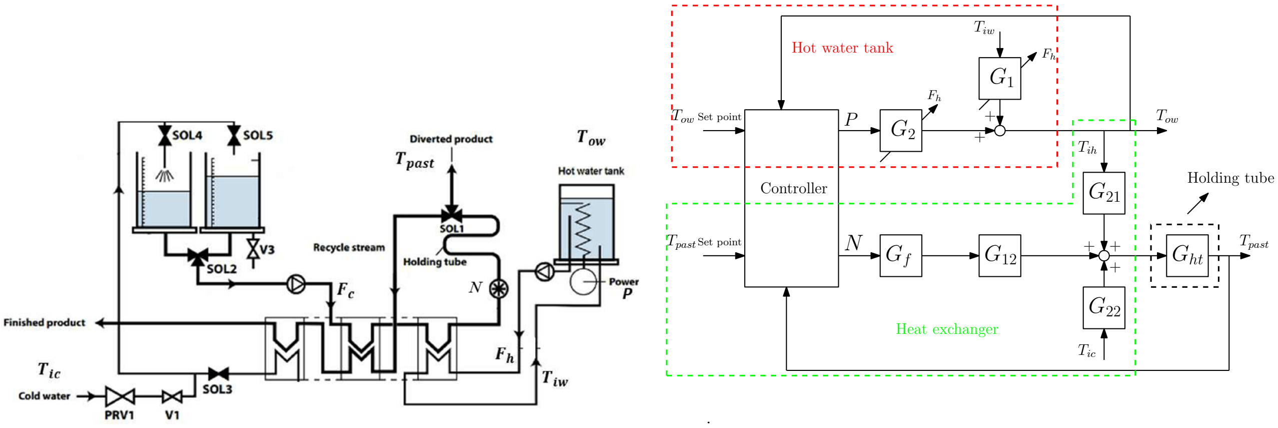

(a) Plant scheme.

(b) The schematic block diagram of the pasteurization system model.

Fig. 1. Plant scheme and control block diagram of the pasteurization plant.

some $a, b \in \mathbb{Z}_+$ *and* $\mathbb{Z}_{\geq c} := \{x \in \mathbb{Z}_+ | x \geq c\}$ *for some* $c \in \mathbb{Z}_+$*. Moreover,* $\|.\|$ *denotes the spectral norm for matrices. The superscript* $`T'$ *represents the transpose and operators* $<, \leq, =, >, \geq$ *denote element-wise relations of vectors.*

2. Problem Statement

2.1. Pasteurization System. The considered pasteurization process is the small-scale plant PCT-23 MKII, manufactured by Armfield (UK) (Armfield, 2015). The system emulates an industrial high-temperature short-time (HTST) pasteurization process. The goal of this process is to heat and keep the product, which is typically a liquid, at a predetermined temperature for a minimum time. Throughout the pasteurization process, the liquid is pumped at a predetermined flow rate from one of two storage tanks to an indirect plate heat exchanger. The water heat is transferred to the product inside the first phase of the heat exchanger. The raw product is heated to an intermediate temperature by using missed energy from the pasteurized product. Then, this product is heated from that middle temperature to the full-pasteurization temperature in the second phase, while using a hot-water flow F_h coming from a closed circuit with a heater. The temperature T_{past} at the output of the holding tube is used to monitor the product temperature after the pasteurization process. Finally, the product is cooled in the third phase of the heat exchanger, where the remaining heat is recuperated. The last phase does not add anything new to the considered model. For this reason, it was not considered in this paper.

2.2. Control-oriented Model. The control-oriented pasteurization model is represented in terms of behavioral equations of each subsystem, consisting of power, water pump, heat exchanger and hot water tank. According to Fig. 1a, the controlled inputs are the power of the electrical heater, P, and the pump rotational speed of the second pump, N, respectively. The input temperature of the water heater, T_{iw}, and the temperature of cold water, T_{ic}, are measured non-controlled inputs (disturbances). Figure 1b shows a block diagram of the simulation model of the pasteurization process, supplied with the benchmark, containing the feedback loops corresponding to the hot-water flow and power of the electrical heater. The dynamic model of the pasteurization plant presented in Fig. 1b is obtained from experimental data considering first order with delay transfer functions (Ibarrola *et al.*, 1998; Ibarrola *et al.*, 2002). The reader is referred to this reference to obtain the values for the parameters. Finally, to design the MPC controller, this model is discretized and expressed in state space form

$$x_{k+1} = Ax_k + Bu_k + Ed_k, \tag{1a}$$

$$y_k = Cx_k, \tag{1b}$$

where $x \in \mathbb{R}^{n_x}$ is the state vector including hot-water flow, F_h, hot-water tank temperature, T_{ow} and pasteurization temperature, T_{past}, $u \in \mathbb{R}^{n_u}$ is the vector of manipulated variables that includes the electrical power of the heater P and the pump rotational speed N, $d \in \mathbb{R}^{n_d}$ is the vector of measured disturbances that include input temperature of the water heater, denoted by T_{iw}, and the temperature of cold water, denoted by T_{ic}. Finally, $y \in \mathbb{R}^{n_y}$ is the vector of controlled variables that include pasteurization temperature, denoted by T_{past}. Moreover, A, B, E and C are time-invariant matrices of suitable dimensions. The state-space matrix A, input matrix B, disturbance matrix E and output matrix C of the model in (1) can be represented in the discrete-time domain as (2), where K and τ are a static gain and a time constant, respectively, and the subindices are related to the first

$$A = \begin{bmatrix} 1+\frac{-T_s}{\tau_1} & 0 & 0 & 0 & 0 & 0 & 0 \\ 0 & 1+\frac{-T_s}{\tau_2} & 0 & 0 & 0 & 0 & 0 \\ \frac{T_sK_{21}}{\tau_{21}} & \frac{T_sK_{21}}{\tau_{21}} & 1+\frac{-T_s}{\tau_{21}} & 0 & 0 & 0 & 0 \\ 0 & 0 & 0 & 1+\frac{-T_s}{\tau_{12}} & 0 & \frac{T_sK_{12}}{\tau_{12}} & 0 \\ 0 & 0 & 0 & 0 & 1+\frac{-T_s}{\tau_{22}} & 0 & 0 \\ 0 & 0 & 0 & 0 & 0 & 1+\frac{-T_s}{\tau_f} & 0 \\ 0 & 0 & 0 & \frac{T_sK_{ht}}{\tau_{ht}} & \frac{T_sK_{ht}}{\tau_{ht}} & \frac{T_sK_{ht}}{\tau_{ht}} & 1+\frac{-T_s}{\tau_{ht}} \end{bmatrix},$$

$$B = \begin{bmatrix} 0 & 0 \\ \frac{T_sK_2}{\tau_2} & 0 \\ 0 & 0 \\ 0 & 0 \\ 0 & \frac{T_sK_{12}}{\tau_{12}} \\ 0 & 0 \\ 0 & 0 \end{bmatrix}, \quad E = \begin{bmatrix} \frac{T_sK_1}{\tau_1} & 0 \\ 0 & 0 \\ 0 & 0 \\ 0 & 0 \\ 0 & \frac{T_sK_{22}}{\tau_{22}} \\ 0 & 0 \\ 0 & 0 \end{bmatrix}, \quad C = \begin{bmatrix} 1 & 1 & 0 & 0 & 0 & 0 & 0 \\ 0 & 0 & 0 & 0 & 0 & 0 & 1 \end{bmatrix}. \tag{2}$$

order plus delay transfer functions of each subsystem (see Fig. 1b) detailed in (Ibarrola *et al.*, 1998; Ibarrola *et al.*, 2002).

2.3. Operational Control. As previously mentioned, the main goal of the pasteurization process is to guarantee that the pasteurization temperature is reached and maintained as close as possible to the set-point value for a per-established time. At the same time, reduction of energy consumption and health management of the system expressed should be achieved by formulating a multi-objective control problem. MPC is a suitable technique to control a pasteurization system due to its capability to deal efficiently with dynamically constrained systems and predict the proper action to achieve the optimal performance according to the user-defined cost function. The control goal can formulated as the minimization of a convex multi-objective cost function which includes the economic and safety system operation objectives. This optimization problem should be solved considering as constraints the mathematical model of the pasteurization system (1) and the operational constraints defined by

$$x_k \in \mathbb{X} \triangleq \{x_k \in \mathbb{R}^{n_x} \,|\, \underline{x} \le x_k \le \overline{x}\}, \quad \forall k, \tag{3a}$$

$$u_k \in \mathbb{U} \triangleq \{u_k \in \mathbb{R}^{n_u} \,|\, \underline{u} \le u_k \le \overline{u}\}, \quad \forall k, \tag{3b}$$

where vectors $\underline{x} \in \mathbb{R}^{n_x}$ and $\overline{x} \in \mathbb{R}^{n_x}$ determine the minimum and maximum possible state values of the system, respectively. Also $\underline{u} \in \mathbb{R}^{n_u}$ and $\overline{u} \in \mathbb{R}^{n_u}$ determine the minimum and maximum possible value of manipulated variables, respectively.

Thus, the MPC controller design is based on the solution of the following finite-time horizon optimization problem (FHOP):

$$\min_{\mathbf{u}_k} \sum_{i=0}^{N_p-1} \|x_{k+i|k}\|_{w_1}^p + \|u_{k+i|k}\|_{w_2}^p + \|\Delta u_{k+i|k}\|_{w_3}^p, \tag{4a}$$

subject to:

$$x_{k+i+1|k} = Ax_{k+i|k} + Bu_{k+i|k} + Ed_{k+i|k}, \tag{4b}$$

$$u_{k+i|k} \in \mathbb{U}, \tag{4c}$$

$$x_{k+i|k} \in \mathbb{X}, \tag{4d}$$

$$(x_{k|k}, u_{k-1|k}, d_{k|k}) = (x_k, u_{k-1}, d_k), \tag{4e}$$

for all $i \in \mathbb{Z}_{[0,N_p-1]}$, where $\mathbf{u}_k = \{u_{k+i|k}\}_{i\in\mathbb{Z}_{[0,N_p-1]}}$ is the decision sequence, with $\mathbf{u}_k$ being the sequence of controlled inputs. Furthermore, p denotes the norm used for this paper is squared norm, $\Delta u_{k+i|k} = u_{k+i|k} - u_{k+i-1|k}$ are the input increments and the weighting matrices $w_1 \in \mathbb{R}^{n_x \times n_x}$, $w_2 \in \mathbb{R}^{n_u \times n_u}$ and $w_3 \in \mathbb{R}^{n_u \times n_u}$ are used to establish the priority of the different control objectives.

Moreover, $\mathbf{u}_k^\star$ denotes the optimal solution of (4) at time step k. According to the MPC receding horizon philosophy, only the first optimal control input is applied, i.e., $u_k = u_{k|k}^\star$. Then, the new measurements are used to update the initial conditions (4e) and then the optimization problem (4) is solved again using the receding horizon principle.

3. Rainflow Counting Algorithm (RFC)

The damage accumulation process on a component produced by cyclic loading is known as $fatigue$. Fatigue is as frequent cause of failure in industrial machinery such as pumps (Ocampo, 2008). In reality, fatigue failure occurs because of the application of fluctuating stresses that are much lower than the stress required causing failure during a single application of stress (Fonte *et al.*, 2015). The common recognized and used measure for fatigue damage estimation is the so-called rainflow counting (RFC) method. RFC algorithm, first introduced by Endo *et al.* (1967), has a complex consecutive and nonlinear structure in order to analyze ideal sequences of loads into cycles. Ordinarily, to compute a lifetime estimate from a given structural stress input signal, the RFC method is exerted by computation cycles and maxima, jointly with the Palmgren-Miner rule to calculate the expected damage. The input signal is received from time signal of the loading parameter of interest, such as torque, force, strain, stress, acceleration, or deflection (Lee, 2005). Figure 2 shows the rain-flow counting procedure.

There are several types of RFC algorithms with different rules proposed by Rychlik (1987) and Downing and Socie (1982), which, at the end, yield in quite similar results. The RFC algorithm used in this paper is presented in Niesłony (2009). This algorithm computes the stress for each rainflow cycle in four steps:

- the stress history is converted to an extremum sequence of alternating maxima and minima of stress;
- for each local maximum M_j, the left (m_j^-) and right (m_j^+) regions where all stress values are below M_j are identified;
- the minimum stress value is $m_j = min\{m_j^-, m_j^+\}$;
- the equivalent stress per rainflow cycle s_j related to M_j is granted by either the amplitude $s_j = M_j - m_j$ or the mean value $s_j = \frac{M_j - m_j}{2}$.

In most of the materials, there is an explicit relationship between the number of cycles and cycles of failure, which is known as $S - N$ or Wöhler curves, whereas the damage D is calculated by using the $S - N$ curve at each stress cycle (Hammerum *et al.*, 2007). An often-used model for $S - N$ curve is

$$s^{c_w} N = K_{sp}, \tag{5}$$

where c_w and K_{sp} are material specific parameters and N is the number of cycles to failure at a given stress amplitude s. The damage imposed by a stress cycle with a range s_j is computed as

$$D_j \equiv \frac{1}{N_j} = \frac{1}{K_{sp}} s_j^{c_w}. \tag{6}$$

Then, the total damage under the linear accumulation damage (Palmgren-Miner) rule is given as

$$D_{ac} = \sum_{j=1}^{\lambda} \frac{1}{N_j} = \sum_{j=1}^{\lambda} \frac{1}{K_{sp}} s_j^{c_w}, \tag{7}$$

for damage increments D_{ac} associated to each counted cycle, where N_j is the number of cycles of failure associated to the stress amplitude s_j and the number of all counted cycles λ. These sequences are presented in Fig. 3. On the top-left and top-right part of Fig. 3, the input stress and the same signal converted into a sequence of maxima and minima are shown, respectively. The instantaneous damage and the accumulated damage are displayed in the bottom part of Fig. 3.

For real-time systems, applying the customary rainflow counting algorithm is quite challenging and computationally heavy. Considerable amounts of data must be stored and provided periodically to obtain a quantity of data in equivalent regular cycles. Besides, the algorithm must be applied to a stored set of data. One of the objectives of this paper is to analyze the fatigue due to pump load of the pasteurization system. Loads in the pump structure arise from several factors, the typical reason for pump failure is bearing damage. However, pressure and pump rotational speed are two damage factors that have the greatest influence on the shaft bearing life. Both variables could be chosen as stress indicators for the pasteurization pump. In this paper, the rotational speed of the pump is used as stress for RFC damage estimation.

Utilizing the RFC algorithm, the accumulated damage is obtained as a function of the cycles of the pump rotational speed stress signal. In order to have available an accumulated damage variable that can be integrated with a linear MPC model, a simplified approach to compute fatigue on time series signal is proposed based on the RFC theory. The outcome of this approach is that the accumulated damage is obtained as a function of time instead of the number of cycles. The proposed approach finds the changes of the sign that correspond to a cycle in the stress time signal. The obtained function at each time instant k is the following:

$$D_k = \begin{cases} 0 & \text{if} \quad I_k = I_{k-1}, \\ \frac{1}{K_{sp}} s_k^{c_w} & \text{if} \quad I_k \neq I_{k-1}, \end{cases} \tag{8}$$

where s_k is a stress at time k defined as

$$s_k = \frac{1}{L} \sum_{q=k-L}^{k} N_{s,q}, \tag{9}$$

L is the number of samples per cycle, N_s is the pump rotational speed moment, q is the difference between the number of samples per cycle and time instant and I_k is the signal adapted to indicate cycle, i.e.,

$$I_k = N_{s,k} - s_k. \tag{10}$$

Then, the accumulated damage is calculated by

$$D_{acc,k} = D_{acc,k-1} + D_k. \tag{11}$$

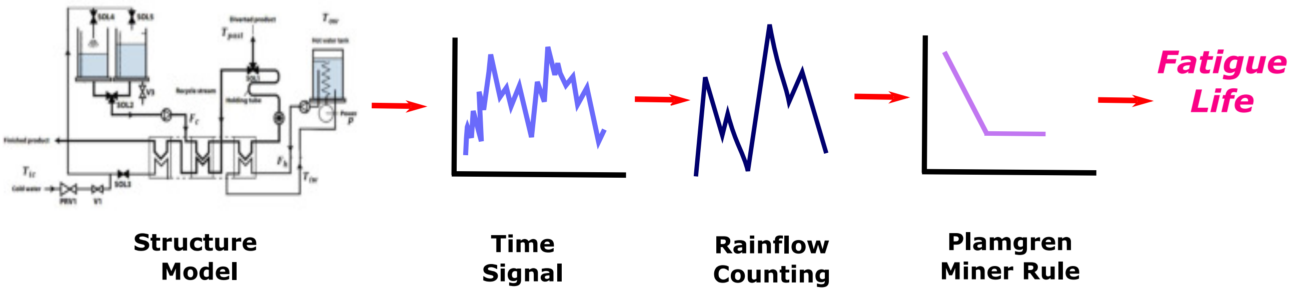

Fig. 2. Rainflow counting damage procedure.

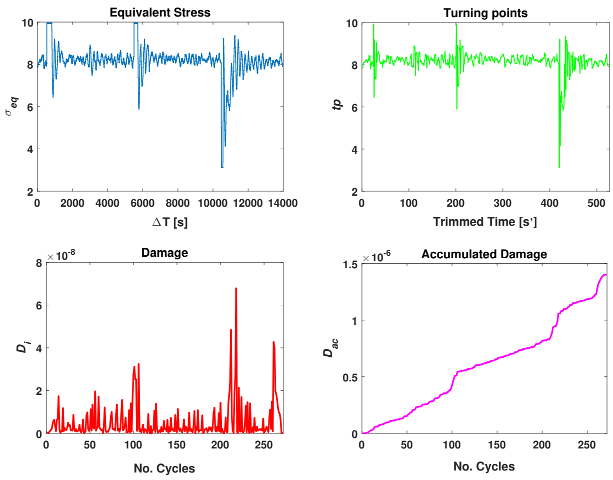

Fig. 3. Rainflow counting damage estimation.

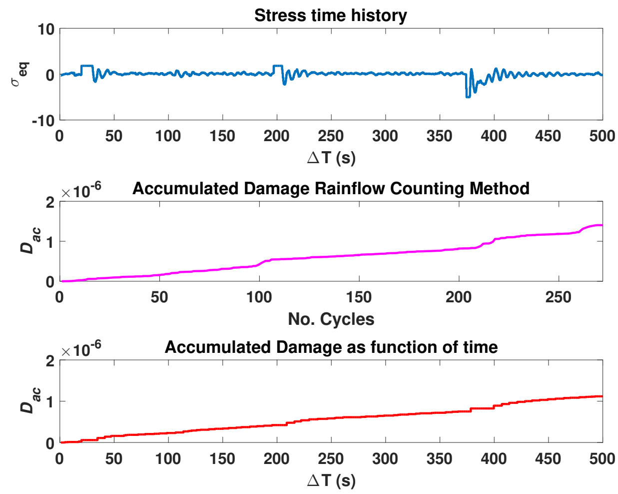

Fig. 4. Accumulated Damage Comparison.

Note that, at the end of the scenario, the accumulated damage based on the function of time and rainflow-counting method is practically the same. Figure 4 indicates the accumulated damage value obtained with each one. The small difference depends on the fact that the damage obtained by the RFC technique is represented in terms of the cycles while the other is a function of time. The degradation procedure of the pasteurization pump can be characterized by using the water pump rotational speed sensor information. In order to decrease the accumulated damage, a new objective is included in the MPC controller that aims at minimizing the pump degradation assessed by means of a linearized RFC model. The slope m of the accumulated damage curve in function of time is computed and then employed as one of the parameters in the linear fatigue damage model. According to Rosich and Ocampo-Martinez (2015), an experimental model that relates the values of the pump rotational speed and flow in steady state is used. The model for the pump rotational speed is a linear model with a slope α_1 and a constant value α_0

$$\bar{N}_{s,k} = \alpha_1 u_{F,k} + \alpha_0, \tag{12}$$

where u_F is the hot-water flow. To sum up, a linear fatigue damage model is considered as a relationship between the accumulated damage of the pump and the control signal

$$z_{k+1} = z_k + \frac{m}{L}(\alpha_1 u_{F,k} + \alpha_0), \tag{13}$$

where z_{k+1} is the accumulated damage of the pump. Then, (13) can be included into the control-oriented model of the MPC as a new state and an additional objective is added into the MPC cost function (4) to minimize the accumulated damage. The degree of fitting between the RFC approximation as a function of time presented in (11) and the linear damage model in (13) can be compared in Fig. 5.

4. Health-aware MPC

In this section, two MPC structures are proposed for adding the health-aware objective into the MPC cost function in order to minimize the accumulated damage.

4.1. Design of Single-layer Health-aware MPC Controllers. First, a health-aware MPC controller based on a single-layer scheme is proposed. In this approach,

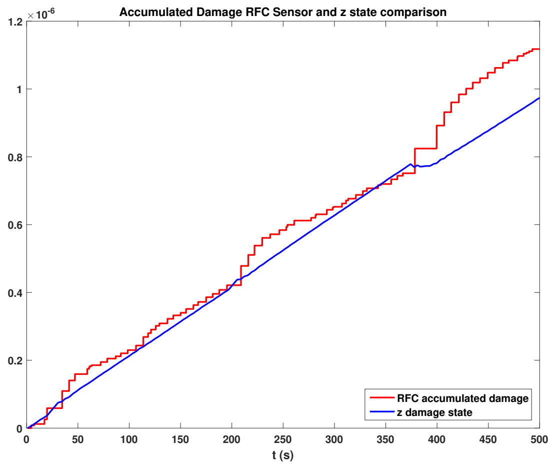

Fig. 5. Accumulated damage RFC as a function of time and z fatigue damage state.

a single-layer MPC that includes a new objective that assesses the system health by means of (13) is considered. The problem formulation of this controller is similar to (4). Taking into account (13), the proposed approach relies on solving the following optimization problem at each time instant k:

$$\min_{\mathbf{u}_k} \sum_{i=0}^{N_p-1} \|e_{k+i|k}\|_{w_1}^p + \|u_{k+i|k}\|_{w_2}^p + \|\Delta u_{k+i|k}\|_{w_3}^p + \|z_{k+i|k}\|_{w_4}^p + \|\xi_{k+i|k}\|_{w_5}^p, \tag{14a}$$

subject to:

$$x_{k+i+1|k} = Ax_{k+i|k} + Bu_{k+i|k} + Ed_{k+i|k}, \tag{14b}$$
$$e_{k+i+1|k} = r_{k+i+1|k} - Cx_{k+i|k} \tag{14c}$$
$$z_{k+1} = z_k + \frac{m}{L}(\alpha_1 u_{F,k} + \alpha_0), \tag{14d}$$
$$T_{ow(k+i|k)} - T_{past(k+i|k)} \geq \zeta + \xi_{k+i|k} \tag{14e}$$
$$u_{k+i|k} \in \mathbb{U}, \tag{14f}$$
$$x_{k+i|k} \in \mathbb{X}, \tag{14g}$$

for all $i \in \mathbb{Z}_{[0,N_p-1]}$, where $e_{k+i|k}$ is the tracking error and $r_{k+i|k}$ is the set-point for the controlled variables while the weighting matrix w_5 is used to manage the penalization of slack variable $\xi \in \mathbb{R}$ that is used for softening the output constraints and ζ is temperature differences between T_{ow} and T_{past} (Rosich and Ocampo-Martinez, 2015). The value of ζ is considered as a design parameter, which was specified by iterative simulations to have a safety temperatures difference. The health-aware objective with the corresponding weight w_4 is appended in the MPC cost function to minimize the accumulated damage. However, the new state in the model of the MPC controller can lead to steady-state offset. Different mechanisms for steady-state offset elimination have been proposed in the literature (González *et al.*, 2008)(Pannocchia and Rawlings, 2003). The strategy used in this paper is introduced in Muske and Badgwell (2002). This method is based on augmenting the process model that includes a constant step disturbance to eliminate the steady-state offset. This disturbance, which is estimated from the measured process variables, is usually considered to be constant in the future and its effect on the controlled variables is eliminated by shifting the steady-state target for a controller. Thus in order to remove the steady state error, the process state-space model is augmented with an integrator as follows:

$$\begin{bmatrix} x_{k+1} \\ e_{k+1} \end{bmatrix} = \begin{bmatrix} A & G_e \\ 0 & I \end{bmatrix} \begin{bmatrix} x_k \\ e_k \end{bmatrix} + \begin{bmatrix} B \\ 0 \end{bmatrix} u_k, \tag{15a}$$
$$y_k = \begin{bmatrix} C & 0 \end{bmatrix} \begin{bmatrix} x_k \\ e_k \end{bmatrix}, \tag{15b}$$

where G_e is a matrix that determines the effect of the disturbances on the states. In this paper, considering (1) and (15a), $G_e = E$. The states of the process model and the unmeasured disturbance model must be estimated simultaneously using the augmented system model (15). The state estimation can be performed either within a stochastic framework using a Kalman filter or within a deterministic framework using a Luenberger observer. In both cases, a gain $L_G = [L_x, L_e]^T$ can be determined using standard methods provided the augmented system is detectable (Kwakernaak and Sivan, 1972). Thus, the steady-state observer equation for a time k is given by

$$\hat{x}_{k+1} = A\hat{x}_k + Bu_{\bar{k}} + G_e\hat{e}_k + L_x[y_k - C(A\hat{x}_k + Bu_k + G_e\hat{e}_k)], \tag{16}$$

$$\hat{e}_{k+1} = \hat{e}_k + L_e\left[y_k - C(A\hat{x}_k + Bu_k + G_e\hat{e}_k)\right], \tag{17}$$

where L_x and L_e are the observer gains that correspond to the states estimation $\hat{x}_k$, and the tracking error $\hat{e}_k$. In this paper, the observer gain L_G that includes L_x and L_e is obtained with the Linear Matrix Inequalities (LMI) pole placement technique (Montes de Oca *et al.*, 2012), which allows to place the eigenvalue of the $A - L_G C$ inside the unit circle using an LMI region

$$\begin{bmatrix} -rX & qX + X^T A - W^T C \\ qX + A^T X - C^T W & -rX \end{bmatrix} < 0, \tag{18}$$

where q and r denote the center and the radius of a circular LMI region, respectively, X is the unknown symmetric matrix and $W = L_G X$. Finally, L_G is obtained as

$$L_G = WX^T. \tag{19}$$

Then, $A - L_G C$ is Schur hence the convergence of the observer in (16) and (17) is guaranteed.

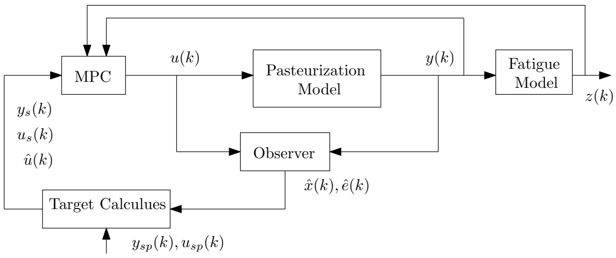

Fig. 6. Representative block diagram of single-layer MPC with fatigue model and linear regulator.

The control scheme presented in Fig. 6 shows the integration of the control with the estimation scheme. In this scheme, there is a MPC regulator block that forces the system to a steady state (x_s and u_s), which represents the accessible steady-state input and state target, respectively. Moreover, a Target Calculus block is in charge to compute these steady-state values, while the variables u_{sp} and y_{sp} correspond to the input and output set-points. Note that the Target Calculus stage does not take into account any economic criterion to be optimized. Moreover, the dynamic control is detached from the set-point calculation: the Targets Calculus block is completely dedicated to obtaining the constant values, while the MPC regulator block is devoted to leading the states $\hat{x}_k$ to its corresponding targets. Then, the optimization problem that must be solved in the regulatory block is as follows:

$$\min_{\tilde{\mathbf{u}}_k} \sum_{i=0}^{N_p-1} \|C\tilde{x}_{k+i|k}\|_{w_1}^p + \|\tilde{u}_{k+i|k}\|_{w_2}^p + \|\Delta\tilde{u}_{k+i|k}\|_{w_3}^p + \|z_{k+i|k}\|_{w_4}^p + \|\xi_{k+i|k}\|_{w_5}^p, \tag{20a}$$

subject to:

$$x_{k+i+1|k} = Ax_{k+i|k} + Bu_{k+i|k} + Ed_{k+i|k}, \tag{20b}$$
$$z_{k+1} = z_k + \frac{m}{L}(\alpha_1 u_{F,k} + \alpha_0), \tag{20c}$$
$$T_{ow,k+i|k} - T_{past,k+i|k} \geq \zeta + \xi_{k+i|k} \tag{20d}$$
$$\tilde{u}_{k-1} = u_{k-1} - u_s, \tag{20e}$$
$$\tilde{x}_k = \hat{x}_k - x_s, \tag{20f}$$
$$u_{min} \leq \tilde{u}_{k+i} + u_s \leq u_{max}, \tag{20g}$$
$$\Delta u_{min} \leq \Delta\tilde{u}_{k+i} \leq \Delta u_{max}, \tag{20h}$$
$$u_{k-1|k} \in \mathbb{U}, \tag{20i}$$
$$x_{k+i|k} \in \mathbb{X}, \tag{20j}$$

for all $i \in \mathbb{Z}_{[0,N_p-1]}$, $\Delta\tilde{u}_{k+i|k} = \tilde{u}_{k+i|k} - \tilde{u}_{k+i-1|k}$ are the input increments, Δu_{min} and Δu_{max} are minimum and maximum value of Δu, where it can be seen that the state and input are led to the targets x_s and u_s in (20f) and (20e), respectively. The role of this part is to steer the shifted states and inputs to zero. Thus, the capability of offset elimination strategy depends on the computation of the targets x_s and u_s. For obtaining this optimal operating point, the following optimization problem is solved:

$$\min_{u_s,x_s} V_k \triangleq \{(y_{sp,k} - y_k^a)^T Q (y_{sp,k} - y_k^a) + (u_{s,k} - u_{sp,k})^T R(u_{s,k} - u_{sp,k})\}, \tag{21a}$$

subject to:

$$x_{s,k+1} = Ax_{s,k} + Bu_{s,k} + G_e\hat{e}_k, \tag{21b}$$
$$y_k^a \triangleq Cx_{s,k}, \tag{21c}$$
$$u_{min} \leq u_{s,k} \leq u_{max}, \tag{21d}$$

where $y_{sp,k}$ stands for the output set-points, and y_k^a is the achievable stationary output. Also, Q and R are positive definite weighting matrices. Following the strategy described in Fig. 6, two optimization problems must be solved at each time instant k.

On the contrary, from (17), the states and disturbances presented by the observer satisfies

$$\hat{x}_{\bar{k}+1} = A\hat{x}_{\bar{k}} + B\hat{u}_{\bar{k}} + G_e\hat{e}_{\bar{k}}, \tag{22a}$$
$$y_{\bar{k}} = C\hat{x}_{\bar{k}}. \tag{22b}$$

Then, subtracting (21b) from (22a) will be

$$(\hat{x}_{\bar{k}+1} - x_{s,k+1}) = A(\hat{x}_{\bar{k}} - x_{s,k}) + B(\hat{u}_{\bar{k}} - u_{s,k}), \tag{23}$$

which relates to the original system considered by the target tracking optimization. The regulator will lead the states $\tilde{x}_k$ to zero, that is

$$(\hat{x}_{\bar{k}+1} - x_{s,k+1}) = 0. \tag{24}$$

Then, subtracting (21c) from (22b)

$$(y_{\bar{k}} - y_{sp}) = C(\hat{x}_{\bar{k}} - x_{s,k}). \tag{25}$$

Finally, from (24) and (25) leads to

$$y_{\bar{k}} = y_{sp}. \tag{26}$$

Therefore, both optimization problems should be solved simultaneous in the case of using an augmented model. However, in the single-layer health-aware MPC scheme since the models of chemical processes are often complex and nonlinear, this leads to long solution times of the optimization problem. Moreover, long optimization horizons and many degrees of freedom increase the computational load. Hence, for chemical processes, one is faced with the trade-off between sub-optimality and computational effort (Alamir, 2009).

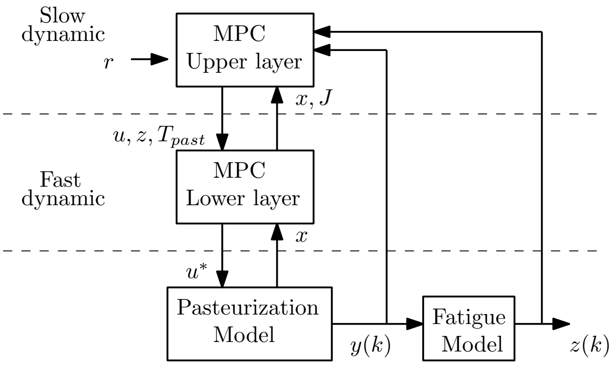

Fig. 7. Representative block diagram of two-layer MPC with fatigue model.

4.2. Design of Multi-layer Health-aware MPC Controllers. In general, the design of multi-layer control architectures can be related to the diverse nature of the control objectives, which would not be able to be coupled into a single-layer architecture. In particular, the control objectives can be ranked in the following way:

- Foremost, the objectives of process operation are to maximize economic benefits and minimize the system degradation. Hence, the process operation is assessed by economic decision criteria and the health-aware objective, which are organized in the objective function of the upper layer optimization. Due to this reason, the degradation takes more time than the tracking trajectory for evaluation, the model considers the slow dynamics of the system.

- Furthermore, the goal of process control is to guarantee a stable operation under the effect of the degradation state and tracking the trajectory, which should be guaranteed by the lower-layer controllers that operate at fast dynamic model.

The control strategy addressed in this part is based on a multilayer (hierarchical) control structure that is shown in Fig. 7. The proposed control system is a two-layer hierarchical architecture, where the solution of the dynamic optimization problem is calculated considering two different time-scales. In the upper layer, an optimization problem is solved with an economic cost function and a health-aware objective. The upper layer considers the slow dynamics of the system and uses larger sampling times than the low layer (slow time scale). Since the accumulation of damage cannot be assessed in a short period of time, the upper layer MPC has been implemented by using a longer prediction horizon, where the sampling time for the discretization of the system is larger than the system in the lower layer. In the lower layer, the tracking controller receives the trajectory calculated by the upper layer and determines the setpoint trajectories for the base-layer control system by considering the faster dynamics of the plant (fast time scale). The current state values are required to provide initial conditions for dynamic real-time optimization (DRTO) and the tracking controller, that have to be estimated by means of measurements from the process. Thus, a time-scale separation of the measurements from the process must be performed, as the upper layer is operating at a lower sampling rate and should only take into account the slow trend in the measurements.

4.2.1. The upper-layer controller. In the optimization problem of the upper layer, the goal is to minimize accumulated damage by inserting (13) as a new state and a new objective in the MPC controller and a trajectory planner calculates a reachable reference y^r as close as possible to the exogenous reference signal r. At the same time, minimizing the economic objective that is the electrical power consumed by the heater is the second control goal of this layer.

Taking into account (13), the proposed approach relies on solving the following optimization problem at each time instant k:

$$\min_{\{u_k, Z_k, x_k^r, \xi_k\}} \sum_{i=0}^{N_{pu}-1} \|r_{k+i+1|k} - y^r_{k+i|k}\|^p_{w_1} + \|u_{k+i|k}\|^p_{w_2} + \|\Delta u_{k+i|k}\|^p_{w_3} + \|Z_{k+i|k}\|^p_{w_4} + \|\xi_{k+i|k}\|^p_{w_5}, \tag{27a}$$

subject to:

$$x^r_{k+i+1|k} = Ax^r_{k+i|k} + Bu_{k+i|k} + Ed_{k+i|k}, \tag{27b}$$
$$y^r_{k+i|k} = Cx^r_{k+i|k}, \tag{27c}$$
$$Z_{k+1} = Z_k + \frac{m}{L}(\alpha_1 u_{F,k} + \alpha_0), \tag{27d}$$
$$T_{ow(k+i|k)} - T_{past(k+i|k)} \geq \zeta + \xi_{k+i|k} \tag{27e}$$
$$u_{k+i|k} \in \mathbb{U}, \tag{27f}$$
$$x^r_{k+i|k} \in \mathbb{X}, \tag{27g}$$

for all $i \in \mathbb{Z}_{[0, N_{pu}-1]}$, and the new objective with the corresponding matrix weight w_4 is appended in the MPC cost function to minimize the accumulated damage. N_{pu} is the prediction horizon of the upper layer and the sampling time of the upper layer is t_u.

4.2.2. The lower-layer controller. The lower-layer controller is tracking the optimal trajectory under the influence of high frequency of the accumulated damage and is executed at sampling time t_l of the process. In the lower-layer, the predictive controller is designed to track the calculated reference that it is obtained from the upper layer. This is derived from the following optimization problem:

$$\min_{u_k} \sum_{i=0}^{N_{pl}-1} \|e_{k+i|k}\|_{w_1}^p + \|\Delta u_{k+i|k}\|_{w_2}^p, \tag{28a}$$

subject to:

$$x_{k+i+1|k} = Ax_{k+i|k} + Bu_{k+i|k} + Ed_{k+i|k}, \tag{28b}$$
$$u_{k+i|k} \in \mathbb{U}, \tag{28c}$$
$$x_{k+i|k} \in \mathbb{X}, \tag{28d}$$

for all $i \in \mathbb{Z}_{[0,N_{pl}-1]}$, where N_{pl} is the prediction horizon of the lower layer. Moreover, $e_{k+i|k} = Cx^r_{k+i|k} - Cx_{k+i|k}$ is the error between the calculated references that are obtained from the upper layer and measured output. Since the accumulated damage should be assessed in a long prediction horizon, $N_{pl} < N_{pu}$ should be established and the sampling time of the upper layer should be grater than on from the lower layer, $t_u > t_l$.

5. Simulation Results

In this section, the performance of the proposed different health-aware MPC schemes is assessed with a case study consisting in a pasteurization plant. This laboratory plant is the small version $(1, 2\text{ m}, 0, 6\text{ m}, 0, 6\text{ m})$ of an industrial pasteurization processes. In addition, the size of the handle tube of pasteurizations pumps is 1.6 mm with wall thickness from 0.5 mm to 8.0 mm bore. The rotor rotational speed is 400 rpm while the flow rate is 200 ml/min.

5.1. Design of the MPC Controller with Health-aware Capabilities and Economic Objectives. In order to test the behavior of the proposed health-aware MPC scheme in two different manners, several simulations were carried out and the results obtained are presented in this part. The operating point for the hot-water flow is chosen as 200 ml/min. The behavior of the controlled temperature T_{past} from the pasteurization plant under the heath-aware hierarchical MPC and single-layer MPC with and without the health-aware objective are presented in Fig. 8 with its corresponding references, while the controlled variable T_{past} tracks the references. In Fig. 9, an evolution of the accumulated damages obtained from multi-layer and single-layer MPC with and without a health-aware objective are provided.

5.1.1. Scenario 1 (Health-aware single-layer MPC). The health-aware MPC is designed as described in Section 4.1, by adding the accumulated damage model presented before, as a new state introduced in (13). In addition, to remove steady state offset that appears with the augmented model in the health-aware MPC is augmented again. Therefore, According to the complete model of the pasteurization system (2), the matrix E is utilized as disturbance in this paper. Now with the disturbance model as follows:

$$x_{n,k+1} = A_s x_{n,k} + B_s u_k + E_s d_k, \tag{29a}$$
$$y_{n,k} = C_s x_{n,k}, \tag{29b}$$

where A_s, B_s, C_s, and E_s are matrices of proper dimensions including accumulated damage and disturbance model given by (13) and (15a). The MPC controller has been implemented considering that the prediction horizon is chosen as $N_p = 400$ and the sampling time is 4 s. The control objective of the MPC controller for the pasteurization system is the pasteurization temperature T_{past} tracking the setpoint, while at the same time, the accumulated damaged evaluated as in (13) and the power of the electrical heater P are minimized. From Fig. 8a and Fig. 9a, it can be seen that the cost and degradations are decreased while the temperature is tracking the references without steady-state offset.

5.1.2. Scenario 2 (Health-aware multi-layer MPC). Alternatively, as discussed in Section 4.2, the health-aware MPC can be implemented using a two-layer hierarchical structure, where the solution of the optimization problem considered in the single-layer scheme is solved at different time scales. The two-layer MPC implemented in the new model is presented by

$$x_{n,k+1} = A_h x_{n,k} + B_h u_k + E_h d_k, \tag{30a}$$
$$y_{n,k} = C_h x_{n,k}, \tag{30b}$$

where the state and output vector are given by $x_n = [x; z]$ and $y_n = [y; z]$, respectively. Moreover, A_h, B_h, C_h, and E_h are state matrices of proper dimensions with included accumulated damage given by (13). The control objectives of the upper layer for the pasteurization system aim at minimizing the accumulated damage evaluated as (13) and reducing the power of the electrical heater as economic objective and at the same time. The appropriate pasteurization temperature T_{past} is calculated in order to save energy and avoid overheating the product. Due to the accumulation of damage can not be assessed in a short horizon, the upper layer MPC has been implemented by using prediction horizon $N_{pl} = 300$, where the sampling time for the discretization of continues state-space model of the pasteurization plant(2) is 120 s. On the other hand, the control objective in the low layer MPC forces that the pasteurization temperature T_{past} is tracking the calculated appropriate pasteurization temperature in the upper layer. The prediction horizon is chosen $N_{pl} = 5$ and sampling time is 4 s. Fig. 8b are the behavior of pasteurization temperature T_{past} with and without the health objective

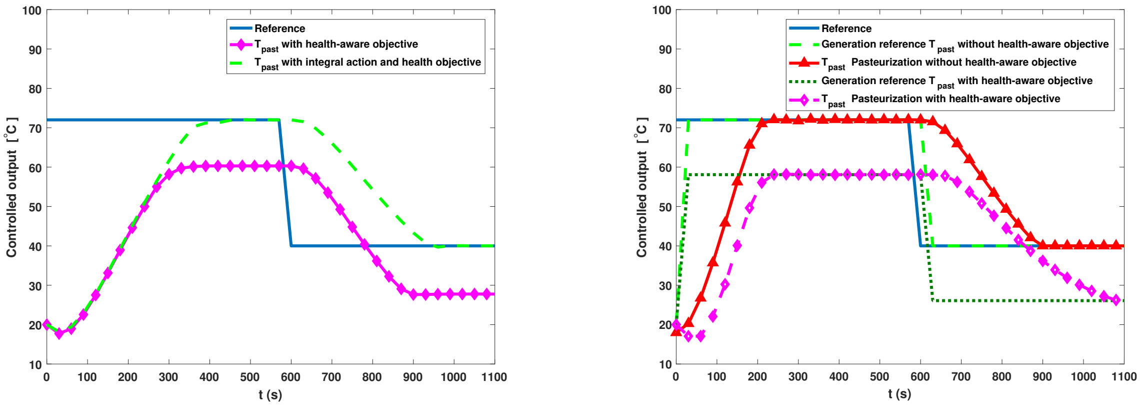

(a) Pasteurization temperature T_{past} in single-layer. (b) Pasteurization temperature T_{past} in multi-layer.

Fig. 8. Evolution of pasteurization temperature T_{past} with and without the health-aware objective in the MPC.

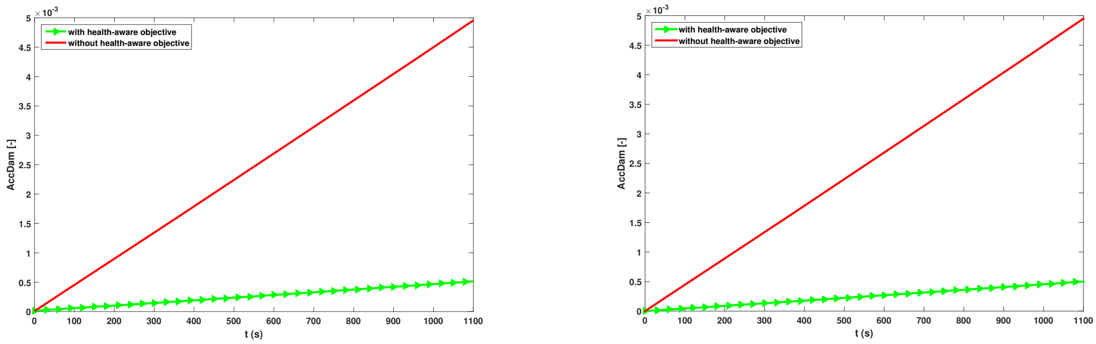

(a) Accumulated damages by single-layer structure. (b) Accumulated damages by multi-layer structure.

Fig. 9. Evolution of accumulated damages with and without health-aware objective in the MPC.

are presented. Moreover, the reduction of accumulated damage under multi-layer MPC scheme is presented in Fig. 9b.

5.2. Results and Comparison Assessment. According to the results, it can be observed that the results of the inclusion of the fatigue objective in single-layer approach and two-layer approach are almost the same (see Fig. 9). In particular, the accumulated damage is mitigated about 88% in both of them. However, from Fig. 10 it can be seen the power of the electrical heater P from the multi-layer MPC is minimized more than the single-layer MPC. This implies that the multi-layer health-aware MPC controller can be achieve better results related to the economic cost objective. While there is some degree of flexibility playing with the temperature set-point for achieving the best result of minimizing accumulated damage in the multi-layer scheme. In order to have better cooperation between the two different control scheme, several simulation with different tunings have been implemented. Finally, the trade-off curves between the health objective and economic cost for single-layer and multi-layer schemes are presented in Fig. 11. Moreover, Fig. 11 shows that independently of the tuning the two-layer scheme is able to produce better results and it can be seen the economic objective in single layer is not optimized as in the case of the multi-layer scheme.

6. Conclusions

In this paper, the integration of MPC with fatigue-based prognosis to minimize the damage of components in a pasteurization plant and the optimization economic objective has been presented. The integration of a system health management module with MPC control has provided the pasteurization plant with a mechanism to operate safely and optimize the trade-off between components lifetime while saving energy, product and time. The MPC controller objective has been modified by adding an extra criterion that takes into account the accumulated damage plus including the economic

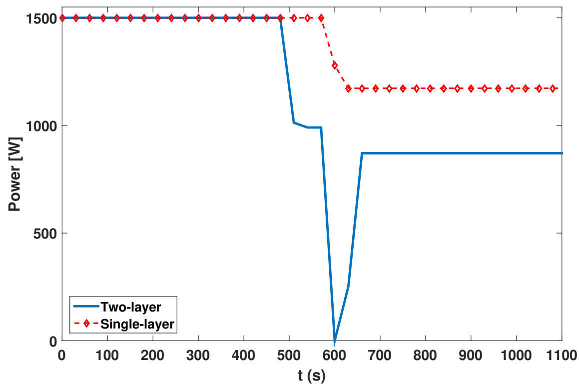

Fig. 10. Evolution of power the electrical heater P in the single-layer and two-layer MPC.

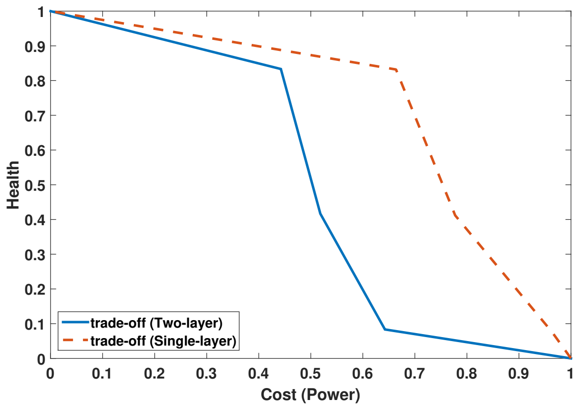

Fig. 11. Trade-off between the health and cost in the single-layer and two-layer MPC over the normalization.

objective. First, a single-layer health-aware MPC controller based on economic optimization by including integral action to eliminate steady state offset by adding extra criterion has proposed. Then, the single layer has been transformed to multi-layer scheme one taking into account the different dynamics of the objectives.

The multi-layer health-aware MPC controller based on two optimization layer has implemented with different time-scale. Both control schemes have been satisfactorily implemented using high-fidelity simulator of a utility-scale pasteurization plant. The results obtained show that there exists a trade-off between the minimization of the accumulated damage and tracking setpoint that manipulated for saving energy. Finally, these control schemes are compared and the results show that the multi-layer control scheme can minimize the economic cost more than the single layer and keeping the same degradation level for the components. As future research, the proposed health-aware MPC controller will be extended by considering that the damage and dynamic models are coupled and integrated with reliability specifications.

Acknowledgment

This work has been partially funded by the Spanish Government (MINECO) through the project DEOCS (Ref. DPI2016-76493-C3-3-R), by MINECO and FEDER through the project HARCRICS (ref. DPI2014-58104-R).

References

Aadaleesan, P., Miglan, N., Sharma, R. and Saha, P. (2008). Nonlinear system identification using Wiener type Laguerre–Wavelet network model, *Chemical Engineering Science* **63**(15): 3932–3941.

Alamir, M. (2009). A framework for monitoring control updating period in real-time nmpc schemes, *Nonlinear Model Predictive Control*, Springer, pp. 433–445.

Alastruey, C. F., De la Sen, M. and García-Sanz, M. (1999). Modelling and identification of a high temperature short time pasteurization process including delays, *Proceedings of the 7th Mediterranean Conference on Control and Automation*, Israel.

Armfield (2015). *Process Plant trainer PTC23-MKII, Instruction Manual*.

de Jesus Barradas-Berglind, J., Wisniewski, R. and Soltani, M. (2015). Fatigue damage estimation and data-based control for wind turbines, *IET Control Theory & Applications* **9**(7): 1042–1050.

Downing, S. D. and Socie, D. (1982). Simple rainflow counting algorithms, *International Journal of Fatigue* **4**(1): 31–40.

Ellis, M., Durand, H. and Christofides, P. D. (2014). A tutorial review of economic model predictive control methods, *Journal of Process Control* **24**(8): 1156–1178.

Endo, T., Mitsunaga, K. and Nakagawa, H. (1967). Fatigue of metals subjected to varying stress—-prediction of fatigue lives, *Preliminary Proceedings of the Chugoku-Shikoku District Meeting, Japanese Society of Mechanical Engineers, Tokyo*.

Fonte, M., Anes, V., Duarte, P., Reis, L. and Freitas, M. (2015). Crankshaft failure analysis of a boxer diesel motor, *Engineering Failure Analysis* **56**: 109–115.

González, A., Adam, E. and Marchetti, J. (2008). Conditions for offset elimination in state space receding horizon controllers: A tutorial analysis, *Chemical Engineering and Processing: Process Intensification* **47**(12): 2184–2194.

Grosso, J. M., Ocampo-Martinez, C. and Puig, V. (2016). Reliability–based economic model predictive control for generalised flow–based networks including actuators' health–aware capabilities, *International Journal of Applied Mathematics and Computer Science* .

Hammerum, K., Brath, P. and Poulsen, N. K. (2007). A fatigue approach to wind turbine control, *Journal of Physics: Conference Series*, Vol. 75, IOP Publishing, p. 012081.

Hrovat, D., Di Cairano, S., Tseng, H. E. and Kolmanovsky, I. V. (2012). The development of model predictive control in automotive industry: A survey, *IEEE International Conference on Control Applications (CCA)*, pp. 295–302.

Ibarrola, J., Guillén, J., Sandoval, J. and García-Sanz, M. (1998). Modelling of a high temperature short time pasteurization process, *Food Control* **9**(5): 267–277.

Ibarrola, J., Sandoval, J., Garcıa-Sanz, M. and Pinzolas, M. (2002). Predictive control of a high temperature–short time pasteurisation process, *Control Engineering Practice* **10**(7): 713–725.

Karimi Pour, F., Ocampo-Martinez, C. and Puig, V. (2017). Output-feedback model predictive control of a pasteurization pilot plant based on an lpv model, *Journal of Physics: Conference Series*, Vol. 783, IOP Publishing, p. 012029.

Karimi Pour, F., Puig, V. and Ocampo-Martinez, C. (2017). Health-aware model predictive control of pasteurization plant, *Journal of Physics: Conference Series*, Vol. 783, IOP Publishing, p. 012030.

Khadir, M. T. (2011). Enthalpy predictive functional control of a pasteurisation plant based on a plate heat exchanger, *International Journal of Modelling, Identification and Control* **13**(1-2): 78–87.

Körber, A. (2014). *Extreme and fatigue load reducing control for wind turbines: a model predictive control approach using robust state constraints*, PhD thesis, Technische Universität Berlin, Berlin.

Kwakernaak, H. and Sivan, R. (1972). *Linear optimal control systems*, Vol. 1, Wiley-interscience New York.

Lee, Y. L. (2005). *Fatigue testing and analysis: theory and practice*, Vol. 13, Butterworth-Heinemann.

Lobos, E. and Momot, M. (2002). Reliability design of complex systems by minimizing the lifetime variance, *International Journal of Applied Mathematics and Computer Science* **12**: 553–557.

Marin, J. C., Barroso, A., Paris, F. and Canas, J. (2008). Study of damage and repair of blades of a 300kW wind turbine, *Energy* **33**(7): 1068–1083.

Miner, M. A. et al. (1945). Cumulative damage in fatigue, *Journal of applied mechanics* **12**(3): 159–164.

Mokhtar, W., Taip, F. S., Aziz, N. and Noor, S. (2012). Process control of pink guava puree pasteurization process: Simulation and validation by experiment, *International Journal on Advanced Science, Engineering and Information Technology* **2**(4): 302–305.

Montes de Oca, S., Puig, V. and Blesa, J. (2012). Robust fault detection based on adaptive threshold generation using interval lpv observers, *International Journal of Adaptive Control and Signal Processing* **26**(3): 258–283.

Musallam, M. and Johnson, C. M. (2012). An efficient implementation of the rainflow counting algorithm for life consumption estimation, *IEEE Transactions on reliability* **61**(4): 978–986.

Muske, K. R. and Badgwell, T. A. (2002). Disturbance modeling for offset-free linear model predictive control, *Journal of Process Control* **12**(5): 617–632.

Niamsuwan, S., Kittisupakorn, P. and Mujtaba, I. M. (2014). Control of milk pasteurization process using model predictive approach, *Computers & Chemical Engineering* **66**: 2–11.

Niesłony, A. (2009). Determination of fragments of multiaxial service loading strongly influencing the fatigue of machine components, *Mechanical Systems and Signal Processing* **23**(8): 2712–2721.

Ocampo, R. (2008). Fatigue failures in pumps-part 1, *World Pumps* **2008**(500): 42–45.

Odgaaard, P. F., Knudsen, T., Overgaard, A., Steffensen, H. and Jørgensen, M. (2015). Importance of dynamic inflow in model predictive control of wind turbines, *IFAC-PapersOnLine* **48**(30): 90–95.

Osgood, C. C. (2013). *Fatigue Design: International Series on The Strength and Fracture of Materials and Structures*, Elsevier.

Pannocchia, G. and Rawlings, J. B. (2003). Disturbance models for offset-free model-predictive control, *AIChE Journal* **49**(2): 426–437.

Rosich, A. and Ocampo-Martinez, C. (2015). Real-time experimental implementation of predictive control schemes in a small-scale pasteurization plant, *Developments in Model-Based Optimization and Control*, Springer, pp. 255–273.

Rychlik, I. (1987). A new definition of the rainflow cycle counting method, *International Journal of Fatigue* **9**(2): 119–121.

Sanchez, H., Escobet, T., Puig, V. and Odgaard, P. F. (2015). Health-aware model predictive control of wind turbines using fatigue prognosis, *IFAC-PapersOnLine* **48**(21): 1363–1368.

Yetendje, A., Seron, M. and De Doná, J. (2012). Robust multisensor fault tolerant model-following mpc design for constrained systems, *International Journal of Applied Mathematics and Computer Science* **22**(1): 211–223.

Fatemeh Karimi Pour received her Biomedical engineering degree from Isalamic Azad University (IAU) of Iran in 2011. In 2014, she received her Master degree in Electrical-Mecatoronic and Automatic Control from Universiti Teknologi Malaysia (UTM). Currently, she is studying Automatic Control, Vision and Robotics as a PhD candidate in Universitat Politècnica de Catalunya (UPC), also she is working at Institut de Robòtica i Informàtica Industrial (CSIC-UPC). Her research interests include constrained predictive control, Health-aware Control, industrial applications.

Vicenç Puig received the telecommunications engineering degree in 1993 and the Ph.D. degree in automatic control, vision, and robotics in 1999, both from Universitat Politècnica de Catalunya (UPC). He is a professor at the Automatic Control Department and a researcher at Institut de Robòtica i Informàtica Industrial, both at UPC. He is the chair of the Automatic Control Department and the head of the research group on advanced control systems at UPC. He has developed important scientific contributions in the areas of fault diagnosis and fault tolerant control, using interval and linear-parameter-varying models using set-based approaches. He has participated in more than 20 European and national research projects in the last decade. He has also led many private contracts with several companies and has published more than 100 journal articles as well as over 350 contributions in international conference/workshop proceedings. He has supervised over 15 Ph.D. dissertations and over 40 Master's theses/final projects. He is currently the vice-chair of the IFAC Safeprocess TC Committee 6.4 (2014–2017). He is the chair of the 3rd IEEE Conference on Control and Fault-Tolerant Systems (SysTol 2016) and the IPC chair of the IFAC Safeprocess 2018.

Carlos Ocampo-Martinez received his Electronics Engineering degree and MSc. degree in Industrial Automation from the National University of Colombia, Campus Manizales in 2001 and 2003, respectively. In 2007, he received the Ph.D. degree in Control Engineering from the Technical University of Catalonia - BarcelonaTech (Barcelona, Spain). Since 2011, he is with the Technical University of Catalunya, Automatic Control Department (ESAII), currently as Associate Professor in automatic control and model predictive control. Since 2014, he is also Deputy Director of the Institut de Robòtica i Informàtica Industrial, CSIC-UPC, a Joint Research Center of UPC and CSIC. His main research interests include constrained model predictive control, large-scale systems management (partitioning and non-centralized control), and industrial applications.